Supporting Information

DeCaen *et al.* 10.1073/pnas.0806486105

SI Text

Mechanism of Reversal of Disulfide Locking. Protein disulfide bonds have a favorable free energy of ≈2 to 5 kcal/mol compared with two free cysteine -SH groups (1, 2). To calculate whether movement of the gating charges of the S4 voltage sensor across the membrane electrical field could generate sufficient energy to reverse disulfide locking, we substituted the Faraday Constant (F = 96,485 Coulomb/mol), the gating charge movement ($z = 3$), the voltage through which the charges move ($\Delta V = 0.2$ Volts = 0.2 Joule/Coulomb), and the relationship 1 kcal = 4184 Joule into the equation $\Delta G^{o} = zF(\Delta V)$. This yields a value of $\Delta G^{o} =$ 13.8 kcal/mol for the energy resulting from the movement of three positive gating charges through an electrical potential difference of 200 mV. This calculation indicates that the electrical energy produced by voltage sensor movement is ≈3-fold greater than the typical energy of a protein disulfide bond, and therefore, that hyperpolarization by 200 mV can indeed drive reversal of disulfide locking.

Although this calculation shows that voltage sensor movement provides sufficient free energy to drive the reversal of disulfide locking, it does not provide information on whether there is sufficient electromotive force generated by this movement to overcome the kinetic barrier for reversal of disulfide locking. Estimates of the force required to physically pull apart a covalent bond range from 1,400 picoNewton (pN) for the Au-S bond to 4,000 pN for the C-C bond (3). These are large forces on the atomic scale. Therefore, we consider it more likely that reversal of disulfide locking involves reduction of the -S-S- bond back to 2 -SH, catalyzed by the force of the electric field polarizing the electrons in the -S-S- bond and separating the two -SH groups after reductive cleavage. Enhancement of reductive cleavage of disulfide bonds by force has been measured directly for reductive cleavage of the intramolecular disulfide bond of titin by DTT (4). Forces from 100 to 400 pN increased the rate of reaction >10-fold (4). Similarly, forces in the range of 25 to 600 pN have strong effects on both the mechanism and rate of disulfide bond reduction catalyzed by thioredoxin (5). To make a comparison with these estimates of the force required to enhance disulfide reduction, we calculated the electromotive force that would be generated by movement of three S4 gating charges through the electric field in the center of the gating pore. Strong evidence supports the idea that the effective electrical length of the gating pore through which S4 moves is shorter than the full 24-Å distance across a lipid bilayer (6, 7). The short distance across the septum of the gating pore has been proposed to generate a "focused field" at the site of gating charge movement (7), and the length of the hydrophobic septum separating extracellular and intracellular solutions has been estimated to be 2–7 Å (8). Using a distance of 5 Å for the width of the hydrophobic septum (8) and the equation $W = FD$, where W is work in Joules, F is force in Newtons, and D is distance, we calculate that movement of the voltage sensor through the septum in gating pore would generate 192 pN of electromotive force, well within the range shown to catalyze reductive cleavage of disulfide bonds. Therefore, we estimate that both the electrical energy and the electromotive force generated by voltage sensor movement are sufficient for voltage-dependent reversal of disulfide locking.

Homology/*De Novo* Modeling of the Voltage-Sensing and Pore-Forming Domains of NaChBac in the Open and Closed States. NaChBac sequence was aligned with $Na_V1.2$, $K_V1.2$, and KvAP channels by using ClustalX software (9). Homology and *de novo* modeling was performed by using the Rosetta-Membrane method (10, 11). The open state $K_V1.2$ structure and model (12, 13) were used as a template to build the open state model of the voltage-sensing domain of NaChBac. The closed state model of the $K_V1.2$ channel was used as a template to build the closed state model of the voltage sensing domain of NaChBac. Loops between the S1-S2, S2-S3, and S3-S4 segments were modeled by using the Rosetta-Membrane *de novo* method (10, 11). No experimental constraints were used during modeling. The side chains in the low-resolution Rosetta method were represented by a pseudo atom, called a "centroid," the position of which calculated for each residue as the average position of the side-chain atoms in residues of the same amino acid identity and with φ and ψ angles in the same 10° × 10° bin and taken from known protein structures in the Protein Data Bank (PDB) (11). 5,000 models were generated followed by model clustering. The best model was chosen as a center of the biggest cluster, defined as having the lowest standard mean deviation value (between positions of $C\alpha$ atoms of all residues) to all other models in a cluster.

1. Siedler F, Rudolph-Bohner S, Doi M, Musiol HJ, Moroder L (1993) Redox potentials of active-site bis(cysteinyl) fragments of thiol-protein oxidoreductases. *Biochemistry* 32:7488–7495.
2. Schmidt B, Ho L, Hogg PJ (2006) Allosteric disulfide bonds. *Biochemistry* 45:7429–7433.
3. Grandbois M, Beyer M, Rief M, Clausen-Schaumann H, Gaub HE (1999) How strong is a covalent bond? *Science* 283:1727–1730.
4. Wiita AP, Ainavarapu SR, Huang HH, Fernandez JM (2006) Force-dependent chemical kinetics of disulfide bond reduction observed with single-molecule techniques. *Proc Natl Acad Sci USA* 103:7222–7227.
5. Wiita AP, *et al.* (2007) Probing the chemistry of thioredoxin catalysis with force. *Nature* 450:124–127.
6. Yang N, George AL, Jr., Horn R (1996) Molecular basis of charge movement in voltage-gated sodium channels. *Neuron* 16:113–122.
7. Starace DM, Bezanilla F (2004) A proton pore in a potassium channel voltage sensor reveals a focused electric field. *Nature* 427:548–553.
8. Chanda B, Bezanilla F (2008) A common pathway for charge transport through a voltage-sensing domain. *Neuron* 57:345–351.
9. Jeanmougin F, Thompson JD, Gouy M, Higgins DG, Gibson TJ (1998) Multiple sequence alignment with Clustal X. *Trends Biochem Sci* 23:403–405.
10. Yarov-Yarovoy V, Baker D, Catterall WA (2006) Voltage sensor conformations in the open and closed states in ROSETTA structural models of K^+ channels. *Proc Natl Acad Sci USA* 103:7292–7297.
11. Yarov-Yarovoy V, Schonbrun J, Baker D (2006) Multipass membrane protein structure prediction using Rosetta. *Proteins* 62:1010–1025.
12. Pathak MM, *et al.* (2007) Closing in on the resting state of the Shaker K^+ channel. *Neuron* 56:124–140.
13. Long SB, Campbell EB, MacKinnon R (2005) Crystal structure of a mammalian voltage-dependent Shaker family K^+ channel. *Science* 309:897–903.

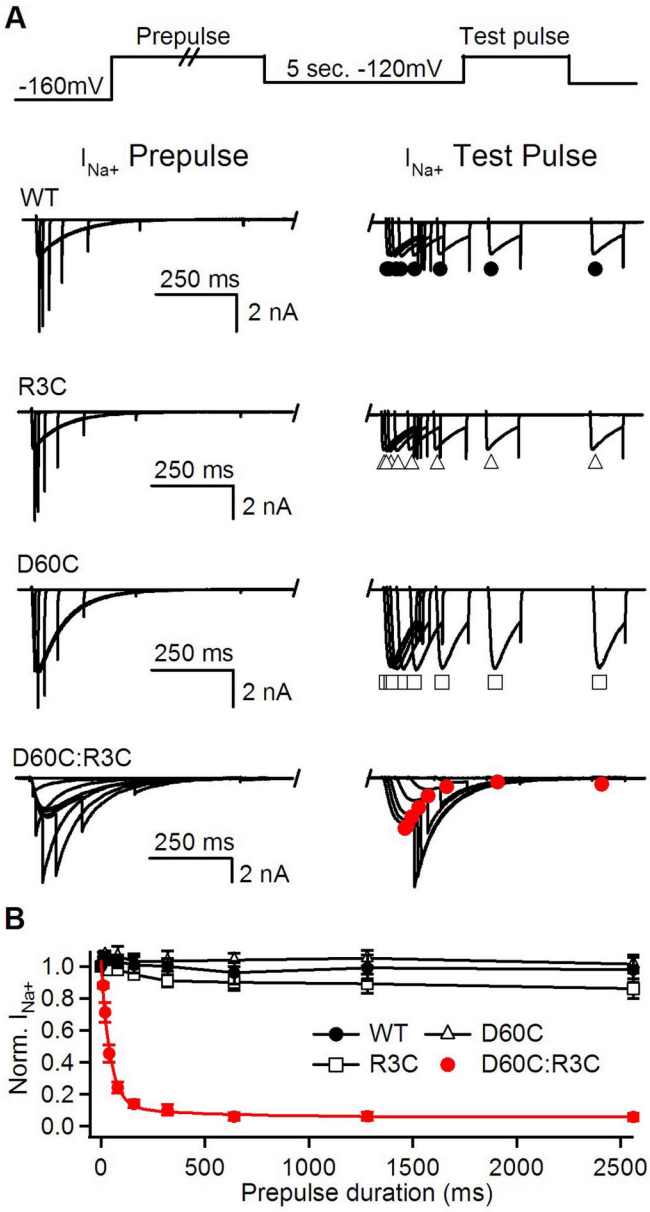

Fig. S1. Original sodium current records for Fig. 3*A*. (*A Top*) The voltage protocol depicting the experiment described in the legend to Fig. 3. (*Lower*) Families of current traces elicited by the prepulses (*Left*) and test pulses (*Right*) for WT, single mutant (D60C and R3C), and D60C:R3C channels. Peak current during the test pulse is indicated by markers. (*B*) Rate of prepulse-dependent inactivation of D60C:R3C channels. Peak test pulse current was normalized to the test pulse current in the absence of a prepulse and mean (±SEM) was plotted versus prepulse duration ($n = 6$).